Microelectronic Engineering 189 (2018) 74–77

Contents lists available at ScienceDirect

Microelectronic Engineering

journal homepage: www.elsevier.com/locate/mee

Research paper

Refined grating fabrication using Displacement Talbot Lithography

Hong Chen [a,b], Li Qin [a], Yongyi Chen [a,*], Peng Jia [a,*], Feng Gao [a,b], Chao Chen [a], Lei Liang [a], Xing Zhang [a], Hongwei Lou [a], Yongqiang Ning [a], Lijun Wang [a]

[a] State Key Laboratory of Luminescence and Application, Changchun Institute of Optics, Fine Mechanics and Physics, Chinese Academy of Sciences, Changchun 130033, China
[b] University of Chinese Academy of Sciences, Beijing 100049, China

A R T I C L E I N F O

Article history:
Received 9 November 2017
Received in revised form 26 December 2017
Accepted 28 December 2017
Available online 29 December 2017

Keywords:
Refined grating fabrication
Displacement Talbot Lithography
Phase shift mask
Photolighography

A B S T R A C T

High-resolution grating areas with none stitching error are in demanding needs but usually expensive and hard to prepare. In this paper, we present a method of making refined grating areas from coarse photolithography mask using Displacement Talbot Lithography (DTL). DTL is relatively simple and low-cost system based on mask photolithography for high-resolution periodic structures over large areas. The grating periods on the ordinary coarse photolithography mask was designed as 3.552 μm. By patterning gratings on Si_3N_4 film deposited on fused silica as intervening phase masks, the final prepared grating periods shrinks 8 times, down to 444 nm. This technology is suitable for producing large area high resolution gratings to reduce the research cost, and can be applied to applications such as DFB laser production, LED substrates preparation and other relative fields.

1. Introduction

Gratings have an ever growing list of applications such as anti-reflection structures, sensor arrays, metamaterial applications, polarizers, plasmonic color filters, spectroscopy and so on [1–8]. The resolution for Bragg gratings in these applications, defined in terms of the lattice constant of the periodic structure, is generally in the 100 nm–1 μm range. Even though projection optical lithography has been served the demands of industry for years, it is not always possible to reach such high resolution, especially considering the depth of focus limitation and high cost. Interference lithography [9,10] is able to break through the limitation of resolution, yet suffers from strict control and stabilization of optical system environment, and especially hard to modify when multiple grating patterns are needed in experimental research conditions. Nano-imprint method [11] requires a high resolution, high cost mask, which is always contaminated by residual polymer. Electron beam lithography method is slow in making large area gratings, meanwhile suffers from the uncertainty of stitching error, which might probably bring a phase shift in Bragg gratings and destruct the optical property.

Displacement Talbot Lithography (DTL) is a recently developed low-cost photolithography technique for patterning high-resolution periodic structures that based on optical masks. By varying the gap between photolithography mask and the wafer corresponding to Talbot length, DTL is able to project periodic patterns easily without contaminating the original mask, because there is no contact between the mask and the wafer when the gap between photolithography mask and the wafer is varying during the whole exposure procedure [12–14]. The time-integrated intensity distribution enables to reach unlimited depth of focus, and for one dimensional grating patterns, the period on the substrate shrinks as half of the period on the mask [13], which makes it possible to produce refined structures from coarse original photolithography mask. In this paper, we present the results of making refined Bragg grating patterns at period of 444 nm from an original coarse photolithography mask periods from 3.552 μm, assisted by two intervening phase shift masks. This technology is suitable for producing high quality large area high resolution gratings, especially when there're different in periods for research purpose, to reduce the cost, and can be applied to applications such as DFB laser production, LED substrates preparation and other relative fields.

2. Simulations and experiments

In order to make the gratings with targeted period of 444 nm, two intervening phase shifting masks are needed to be designed and fabricated. Firstly, we use the coarse photolithography mask with grating patterns of 3.552 μm period to produce a intervening phase shifting mask with grating patterns of 1.776 μm period using DTL, naming intervening phase shift mask-I (IPSM-I). Then, we use IPSM-I to make another phase shifting mask with grating patterns of 888 nm periods naming intervening phase shift mask-II (IPSM-II). Finally, the target 444 nm grating pattern is to be produced by IPSM-II.

For normal incidence illumination of IPSM-I and IPSM-II, we can carefully tune the duty cycle and the depth of the grating, in order to optimize the strongest ±1 order diffraction to interfere, forming a period

* Corresponding authors.
E-mail addresses: chenyy@ciomp.ac.cn (Y. Chen), jiapeng@ciomp.ac.cn (P. Jia).

https://doi.org/10.1016/j.mee.2017.12.018
0167-9317/

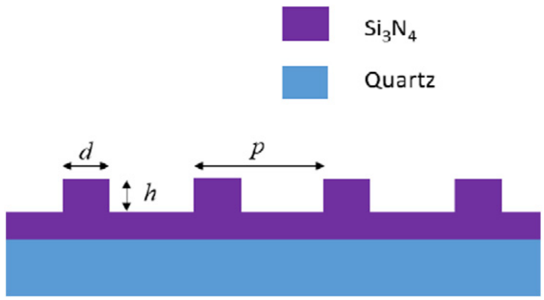

Fig. 1. Schematic showing mask design parameters of the silicon nitride gratings for simulation.

shrunken by half grating pattern independent of the distance from the mask. 440 nm silicon nitride (Si_3N_4) deposited on fused silica (quartz) was chosen thanks to its high refractive index enables the formation of relatively strong 1st diffraction orders and easy processed by inductively coupled plasma (ICP) etching.

In simulation, IPSM-I and IPSM-II are supposed to be illuminated by collimated laser at 377 nm and polarized perpendicular to the grating lines. We name the period of the gratings p, the etching depth of the gratings h, and bulge of the gratings d, as shown in Fig. 1. Then the filling factor is described by d/p. p of IPSM-I is 1.776 μm and p of IPSM-II is 888 nm. h and d/p are varied to see how the intensity of back reflection, 0th and 1st-order diffraction change correspondingly. Simulation was carried out with the help of commercial FEM software COMSOL Multiphysics. Maps of the simulation results illustrating the intensity of back reflection, 0th and 1st order diffraction of IPSM-I are shown in Fig. 2(a), Fig. 2(b) and Fig. 2(c) respectively. Fig. 2(d) gives a specific result demonstrating the intensities at filling factor $d/p = 0.5$. The corresponding maps of the intensities for IPSM-II are given in Fig. 3(a), Fig. 3(b) and Fig. 3(c), demonstrating the back reflection, 0th and 1st order diffraction respectively. Meanwhile Fig. 3(d) gives a specific result demonstrating the intensities at filling factor $d/p = 0.5$.

Inspecting Fig. 2. and Fig. 3. we find that, the maximization of 1st order diffraction and the minimization of the 0th order diffraction can be achieved simultaneously with the same grating parameters: with a grating filling factor d/p of 0.3–0.7 and a grating depth h of 165 ± 20 nm. The intensities of the 0th and 1st order diffraction of the incident light are respectively <5% and ~35%.

Based on the simulation results, IPSM-I was fabricated by a DTL exposure followed by ICP etching from the original coarse Chromium mask, using a commercialize Phable R 100 system supplied by EULITHA. The period shrunk from 3.552 μm to 1.776 μm. Then, IPSM-I was stick to an opaque glass to function as the source mask, and IPSM-II was made following the same procedure. After this step, the grating period shrunk from 1.776 μm down to 888 nm. Finally, target sample was made from IPSM-II, reaching a destination period of 444 nm grating. Fig. 4 gives the SEM pictures of IPSM-I (Fig. 4(a)), IPSM-II (Fig. 4(b)), and the target sample (Fig. 4(c)), as we can see under a same measuring scale, how the lines were doubled step by step. The area of the patterns were designed to be 3.6 mm*1.5 mm. The exposure time was only 175s for IPSM-I and IPSM II, and only 90s for the targeted 444 nm grating pattern. It usually takes 3 hours for electron beam lithography to make such a large area pattern, and to repeat the grating pattern, it will take another 3 hours. Yet by using DTL method, once IPSM II is made out, it can repeat the grating fabrication procedure with a steady exposure time of 90s. This method of making refined gratings is quick and commercially available.

3. Discussion

Ordinary photolithography masks are usually capable of 1 μm line or groove, and Talbot effect considers mostly about the periods of the gratings, and have a large tolerance upon fabrication error. The fabrication tolerance for IPSM-I and IPSM-II are large enough: for etching depth h, the fabrication tolerance reach ±20 nm, and for filling factor d/p, the fabrication tolerance was from 0.3 to 0.7, which are quite easy for processing. The only limitation of refined grating fabrication using DTL

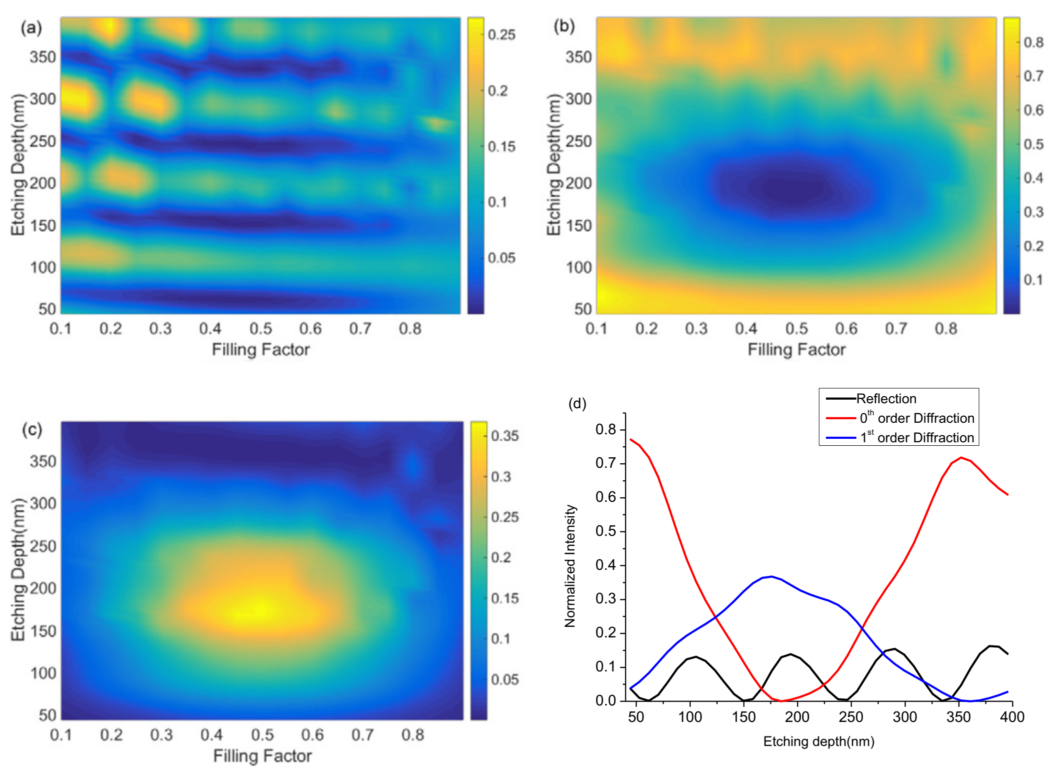

Fig. 2. Simulation results of intensity for back reflection (a), 0th (b) and 1st order diffraction (c) of IPSM-I (period 1.776 μm). (d) demonstrates the intensities at $d/p = 0.5$.

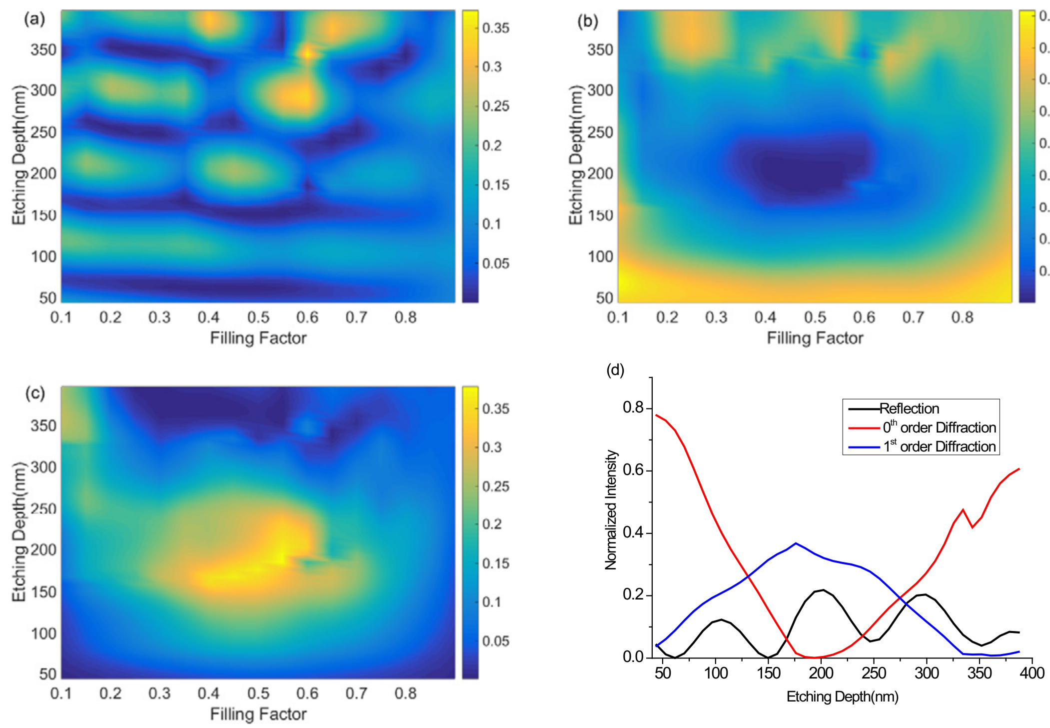

Fig. 3. Simulation results of intensity for back reflection (a), 0th (b) and 1st order diffraction (c) of IPSM-II (period 888 nm). (d) demonstrates the intensities at $d/p = 0.5$.

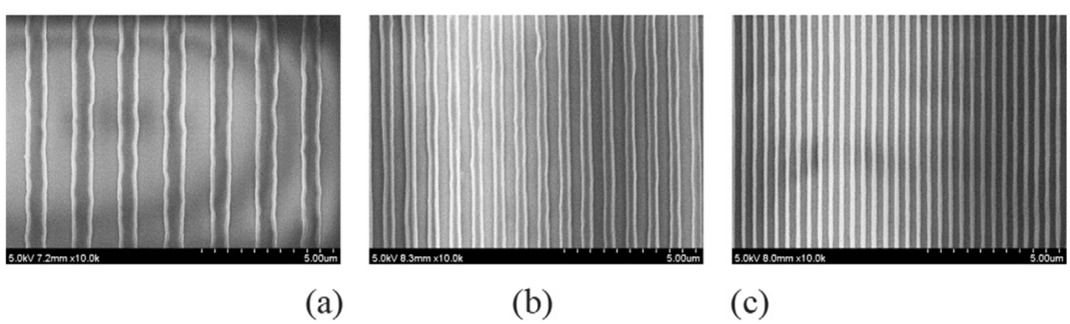

Fig. 4. The SEM pictures of IPSM-I (a), IPSM-II (b), and the target sample (c).

method is dominated by the theoretically limited fabrication period of 188.5 nm under a given wavelength of 377 nm laser source. It is quite possible, but still needs our future effort to further refine the grating period down to 222 nm, which is the first order grating in silicon on oxide materials for 1550 nm wavelength integrated optics.

4. Conclusion

High resolution grating areas with period of 444 nm was fabricated from a 3.552 μm ordinary coarse photolithography Chromium mask by using DTL method to produce two intervening phase shift masks IPSM-I and IPSM-II. This new method is suitable to produce large grating areas with accurate period request and without stitching error, in a low cost way, and especially suitable for grating parameter determination in research.

Acknowledgments

This work was supported by National Natural Science Foundation of China (NSFC) (61234004, 61727822, 51672264, 61674148, 11604328, 61235004, 61505206); National Science and Technology Major Project of China (2016YFE0126800); Frontier Science Key Program of President of the Chinese Academy of Sciences (QYZDY-SSW-JSC006); Natural Science Foundation of Jilin Province (20160520017JH, 20150520089JH, 20160414016GH, 20170623024TC).

References

[1] B. Zhang, Z. Wang, S. Brodbeck, et al., Zero-dimensional polariton laser in a subwavelength grating-based vertical microcavity, Light: Science & Applications 3 (1) (2014), e135.
[2] C. Lu, X. Hu, K. Shi, et al., An actively ultrafast tunable giant slow-light effect in ultrathin nonlinear metasurfaces, Light: Science & Applications 4 (6) (2015), e302.
[3] V.A. Fedotov, J. Wallauer, M. Walther, et al., Wavevector selective metasurfaces and tunnel vision filters, Light: Science & Applications 4 (7) (2015), e306.
[4] J. Yang, Z. Wang, F. Wang, et al., Atomically thin optical lenses and gratings, Light: Science & Applications 5 (3) (2016), e16046.
[5] D. Floess, J.Y. Chin, A. Kawatani, et al., Tunable and switchable polarization rotation with non-reciprocal plasmonic thin films at designated wavelengths, Light: Science & Applications 4 (5) (2015), e284.
[6] L. Wang, X.W. Lin, W. Hu, et al., Broadband tunable liquid crystal terahertz waveplates driven with porous graphene electrodes, Light: Science & Applications 4 (2) (2015), e253.
[7] T. Allsop, R. Arif, R. Neal, et al., Photonic gas sensors exploiting directly the optical properties of hybrid carbon nanotube localized surface plasmon structures, Light: Science and Applications 5 (2016), e16036.
[8] J. Qin, R.M. Silver, B.M. Barnes, et al., Deep subwavelength nanometric image reconstruction using Fourier domain optical normalization, Light: Science & Applications 5 (2) (2016), e16038.

[9] S.R.J. Brueck, Optical and interferometric lithography—nanotechnology enablers, Proc. IEEE 93 (10) (2005) 1704–1721.
[10] T.A. Savas, M.L. Schattenburg, J.M. Carter, H.I. Smith, Large-area achromatic interferometric lithography for 100 nm period gratings and grids, J. Vac. Sci. Technol. B 14 (6) (1996) 4167–4170.
[11] S.Y. Chou, P.R. Krauss, P.J. Renstrom, Imprint of sub-25 nm vias and trenches in polymers, Appl. Phys. Lett. 67 (21) (1995) 3114–3116.
[12] L. Wang, F. Clube, C. Dais, et al., Sub-wavelength printing in the deep ultra-violet region using Displacement Talbot Lithography, Microelectron. Eng. 161 (2016) 104–108.
[13] H.H. Solak, C. Dais, F. Clube, et al., Phase shifting masks in Displacement Talbot Lithography for printing nano-grids and periodic motifs, Microelectron. Eng. 143 (2015) 74–80.
[14] H.H. Solak, C. Dais, F. Clube, Displacement Talbot lithography: a new method for high-resolution patterning of large areas, Opt. Express 19 (11) (2011) 10686–10691.